Available online at www.sciencedirect.com
SCIENCE DIRECT
Polymer 47 (2006) 5678–5690
polymer
www.elsevier.com/locate/polymer

Strain-induced mesophase and hard-elastic behaviour of biodegradable polyhydroxyalkanoates fibers

E.M. Antipov [a,*], V.A. Dubinsky [a], A.V. Rebrov [a], Yu. P. Nekrasov [a], S.A. Gordeev [a], G. Ungar [b]

[a] *Topchiev Institute of Petrochemical Synthesis of Russian Academy of Sciences, Leninskii prospect 29, 119991 Moscow, Russian Federation*
[b] *Department of Engineering Materials, University of Sheffield, Robert Hadfield Building, Mappin Street, S1 3JD Sheffield, UK*

Received 23 March 2005; accepted 24 April 2005
Available online 19 May 2006

Dedicated to Professor David Bassett's retirement.

Abstract

Structure, phase transitions and mechanical properties of fibers of biodegradable bacterial polyester poly(β-hydroxybutyrate) and its random copolymers, prepared by gel-spinning and multistage melt-extrusion, were studied by X-ray diffraction, DSC and mechanical testing. It was found for the first time that as-spun fibers of the homopolymer display pronounced hard-elasticity. They exhibit reversible recovery of sample dimensions on loading and unloading, a behavior typical of hard-elastic fibers. It was also observed that elastic drawing leads to reversible formation of the strain-induced columnar mesophase with a 2D pseudohexagonal arrangement of conformationally disordered chains in addition to the orthorhombic crystalline and amorphous phases of the initial material. In contrast, binary and ternary random copolymers based on poly(β-hydroxybutyrate), being still crystallizable in spite of having relatively high comonomer content, behave like rubbers rather than true thermoplastics.

Keywords: Biodegradable polyhydroxyalkanoates fibers; Structure; Properties

1. Introduction

In the past decades, the necessity of reducing the amount of municipal waste has been well recognized. However, in processing for certain end-use applications such as disposables, packaging and coating, recycling is neither practical nor economical. For such applications plastics are required that will fragment or degrade after use under a wide variety of environmental conditions, including composting. Furthermore, most synthetic plastics originate from non-renewable resources like oil. In certain areas, the use of such plastics could be reduced by application of biopolymers.

Biodegradable macromolecules, have been studied extensively in recent years because, first of all, they offer an environmentally safe alternative to commercial polymeric materials in various practical applications [1]. In particular, poly(hydroxyalkanoates) (PHAs), being among promising substitutes of modern high-volume polymers, are also interesting from the viewpoint of basic research. The advantages of these bacterial aliphatic polyesters are their efficient enzymatic synthesis from renewable raw materials, particularly from wastes of the sugar industry, their excellent biodegradability, biocompatibility, high barrier properties, etc.

Poly(β-hydroxybutyrate) (PHB), the first member of the PHA homologous series, was described as early as the beginning of the 20th century [2]. One of the probable schemes of its bacterial synthesis/degradation routes are shown in Fig. 1. Some TEM micrographs of *Azotobacter* accumulating the polymer inside of the bacteria cell are presented in Fig. 2. At present, polymers with widely variable molecular weight (degree of polymerization from 600 to 15,000) can be obtained from industrial-scale batch cultures. More than 100 copolymers of this class have been described, ranging from hard highly crystalline thermoplastics to elastic materials and soft sticky composites (see, for instance, review [3]).

However, PHB and especially its copolymer derivatives are still relatively expensive materials. The other disadvantage is relatively poor mechanical properties (in particular, brittleness) of their isotropic samples, such as films. This is probably due to the proximity of the glass transition range to ambient temperature ($T_g = +5$ °C for PHB and $-5,\ldots,-10$ °C for the

* Corresponding author. Tel.: +7 95 9554169; fax: +7 95 2302224.
E-mail address: antipov@ips.ac.ru (E.M. Antipov).

0032-3861/$ - see front matter © 2006 Elsevier Ltd. All rights reserved.
doi:10.1016/j.polymer.2005.04.111

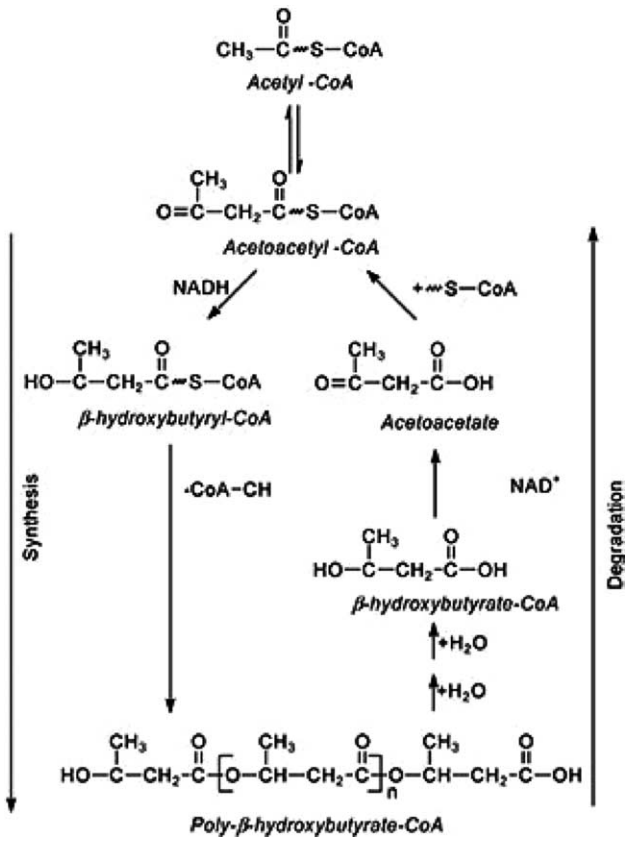

Fig. 1. Schematic representation of the synthesis and degradation reactions of bacterial PHA.

random copolymers). There have been only very few reports on structure and morphology of the oriented state of these polymers. This is primarily due to difficulties in high-temperature processing of such polymers as their melting and thermal degradation temperature ranges overlap [4]. Indications are that PHB may soon become available at a relatively low price in large-scale quantities (see, for example, [5]). Therefore, the only problem remaining to be solved is successful processing.

In addition, until now there have only been a limited number of studies of the effects of processing conditions on structure development and mechanical characteristics of relatively low-crystallinity ($C<20\%$) PHB-based random copolymers. Moreover, papers devoted to their fibers are virtually absent. As is well known, fiber melt-spinning temperature can be significantly reduced by using statistical copolymers rather than PHB homopolymer, while keeping the incipient degradation temperature unchanged. Undesirable decrease in molecular weight during processing can thus be prevented. It is for this reason that we prepared fibers from binary and ternary copolymers for the present study.

As to the processing of the neat PHB homopolymer, as far as we know, apart from our own research, only one successful attempt to produce PHB in the way commonly used in fiber processing industry has been reported. This is the so-called high-speed spinning [6]. Another successful approach is likely to be the gel-spinning technique, originally developed for fiber spinning of ultra-high viscosity ultra-high molecular weight PE (see, for instance, [7]), and proposed for PHB processing for the first time in our group [8].

We use the latter method to produce fibers from PHA, and it seems that we are successful. Because, from a technological point of view, the prepared fibers look very promising, it is important to examine their structure, phase composition and mechanical behaviour in order to control the properties of the resulting material. Below we report some data on such an investigation.

2. Experimental

2.1. Materials

The PHB under investigation was prepared through biosynthesis in Russia by Dr Bonartseva [9], who kindly provided us with samples for this study,

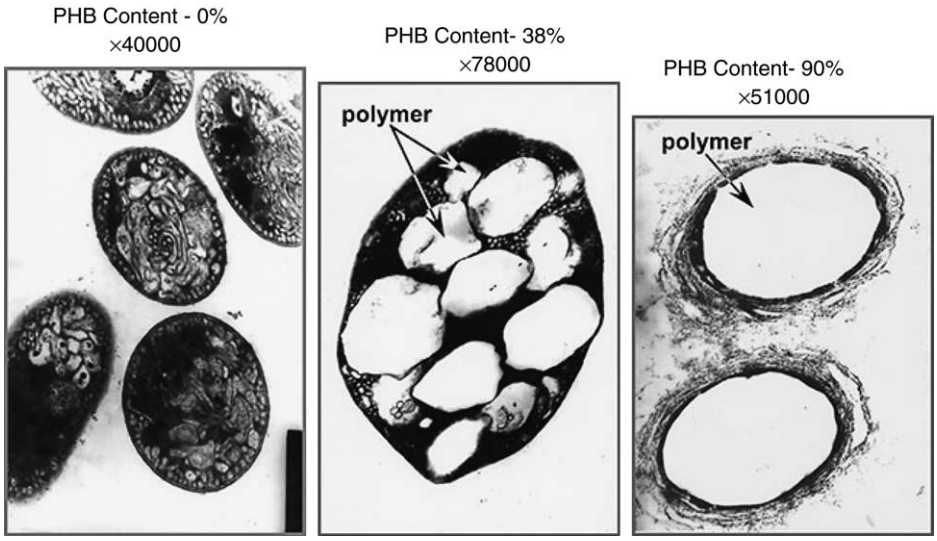

Fig. 2. Transmission electron micrographs of ultrathin sections of *Azotobacter*.

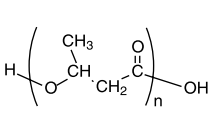

type A

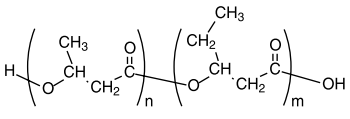

type B

The extraction of the target polymer from biomass included the following stages: repeated dissolution in chloroform, separation from cellular residues via filtration, and a further recovery of polymer from its solution via precipitation with isopropanol.

As estimated by the viscosity measurements, the average molecular weight of the as-synthesized samples of homopolymer PHB is equal to 3.3×10^5; according to X-ray data, the degree of crystallinity is ~70%. Fibers prepared from this polymer under different processing conditions will be referred to below as A1, A2, etc.

We have also examined the commercial random copolymer with a trademark 'Biopol', which was kindly provided by Metabolix Ltd (USA). It contained about 90 mol% of PHB and 10 mol% of the second member in the PHA homologous sequence, poly(hydroxyvalerate) (PHV). The viscosity-average molecular weight of the original materials was 3.5×10^5, and the crystallinity, according to WAXS data, was ~50%. Fibers prepared from this copolymer will be referred to as B1, B2, etc.

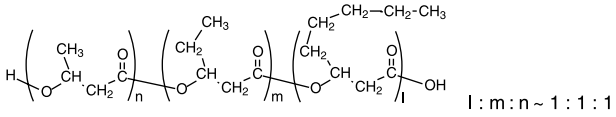

type C

The terpolymer under study was also prepared by biosynthesis in Russia by Prof. Dr Volova [10], who kindly provided the samples. According to NMR data, this copolymer contains approximately equal amounts of PHB, PHV, and poly(hydroxyoctanoate) (PHO); its molecular weight is $M\sim4\times10^5$, as determined by viscometry, and the crystallinity is ~15% according to WAXS data. The melting point of PHA copolymer, as measured by DSC, is ~60 °C. This allows melt-processing of this copolymer without thermal degradation, which becomes noticeable only at temperatures higher than 170 °C. Fibers prepared from this material will be referred to as C1, C2, etc.

2.2. Fiber preparation

In order to overcome the problems caused by the overlap of melting and thermal degradation temperatures for PHB homopolymer, German scientists developed the high-speed spinning technology [6] that allowed a marked reduction in exposure time of the polymer to high temperatures during melt-processing. In contrast, we have adopted and improved two other routes. The first approach is a variation of the traditional melt extrusion and spinning method, consisting of several stages discussed in detail in [11]. The processing parameters in this procedure need to be tightly controlled at every stage in order to minimize polymer degradation. This method is most effective for random PHA copolymers, with melting temperatures lower than those of the PHB homopolymer [12].

The second route [8] is an adaptation of the gel-spinning technology for processing of PHAs. This approach has turned out to be very successful for the treatment of PHB homopolymer or its copolymers with relatively small amount of comonomer, where melting and degradation temperatures overlap. The method allows a decrease in processing temperature to a safe level, enables a broadening of the temperature window suitable for processing, and allows time for pre-orienting the macromolecules prior to the onset of extensive crystallization.

It is important to note that the optimization of both of the proposed technological procedures involves a variation of a number of different parameters strongly affecting the properties of the resulting fibers. According to a rough estimate, there are at least 15 such parameters (solvent type, polymer concentration in the gel, temperatures of extrusion and spinning, draw ratio, etc.). This does not include the initial preparation of the nascent polymer and its specific characteristics. Thus, in order to complete the overall optimization procedure, one has to carry out a vast number of systematic test-experiments. Such engineering development studies are outside the scope of the present publication.

2.3. Methods

WAXS and SAXS analyses were performed using a 12-kW Rigaku rotating anode generator (Japan) equipped with a GADDS 2D-area detector by Bruker AXS (Germany) and a flat graphite monochromator in the primary beam (Cu K_α irradiation, $\lambda=0.154$ nm). The sample was fixed either by a standard holder or by a specially designed one equipped with clamps keeping the fiber length isometric (for samples under loading). For equatorial and meridional scans, a standard Rigaku goniometer with slit collimation and Ni–filtered Cu K_α-irradiation was used.

2θ Angular positions and halfwidths of Bragg reflections were measured using the EVA-Diffrac-Plus software (Bruker AXS). The azimuthal peak profiles were approximated by Gaussian and Lorentzian curves using Origin 7.5 software.

Mechanical properties were studied using an Instron-1121 universal tensile machine (UK); the gauge length of the samples was 10 mm and the strain rate was 20 mm/min. DSC measurements were performed with a Mettler Toledo Star System (Switzerland) at heating and cooling rate of 10 °C/min. NMR measurements were carried out with a Bruker AG spectrometer (Germany) operating at a frequency of 125 MHz.

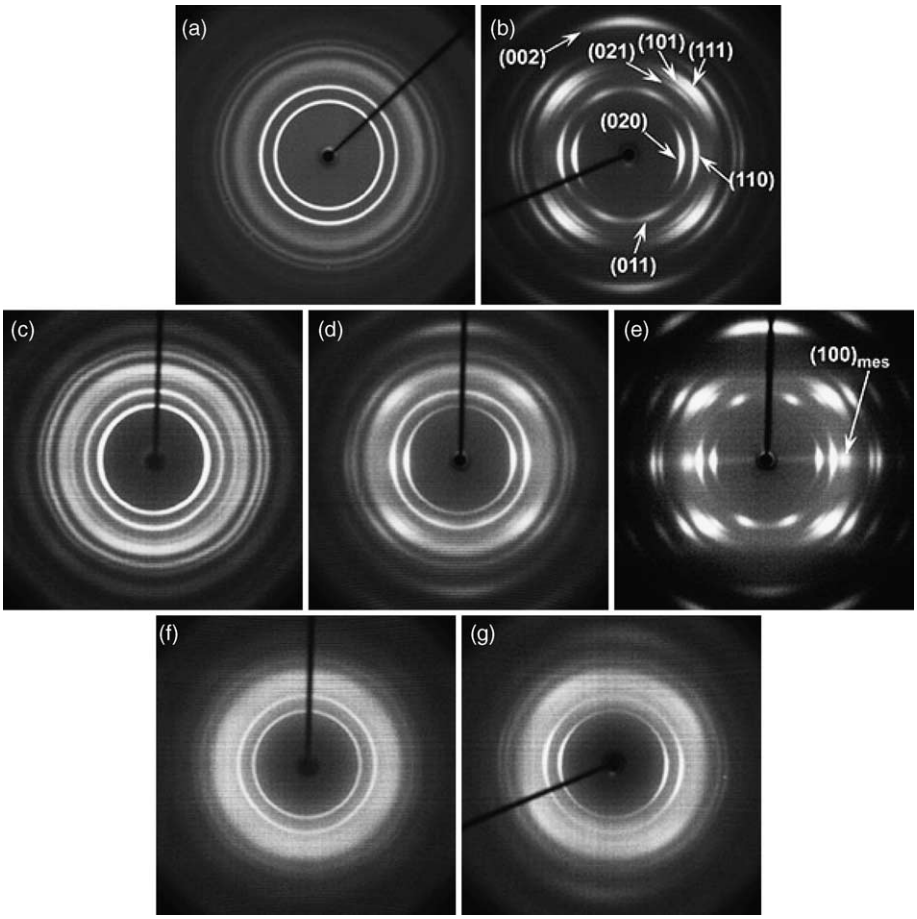

Fig. 3. WAXS patterns of isotropic PHB (a) and its gel-spun fiber (b), of isotropic Biopol (c) and its melt-spun fibers with draw ratios $\lambda = 5$ (d) and 10 (e), prepared under different processing conditions, as well as of low-crystallinity isotropic (f) and oriented (g) samples. Fiber axis is vertical.

3. Results and discussion

3.1. Structural and phase characteristics and mechanical properties of PHA fibers

Fig. 3 shows X-ray diffraction patterns recorded for all three families of polymers under study: an isotropic sample of PHB and its gel-spun fibers prepared according to [8] (type A), as well as for an isotropic sample and melt-spun fibers of relatively high crystallinity (type B) and relatively low crystallinity (type C) copolymers prepared according to [11]. The Bragg reflections for both isotropic and oriented specimens can be indexed on an orthorhombic lattice [13], thus one can state that the type of crystalline lattice remains unaffected by the processing route. Some crystallographic data obtained for homo- and co-polymer fibers prepared are given in Table 1.

It is important to note that under certain processing conditions the resulting fibers exhibit a third phase in addition to the crystalline and amorphous phases. This is indicated by the appearance of a new single reflection at $2\theta \sim 18.7°$ ($d \sim 0.47$ nm) on the equatorial line of the X-ray pattern (Fig. 3(e)). Similar observations were made earlier in [14], where this new component was identified as the 'β-phase' with hexagonal packing of macromolecules built of 'stretched' polymer chains

Table 1
Some crystallographic data for PHA fibers under study

Fiber		HW_{020} (°)	F	A (nm)	b (nm)	c (nm)	C (%)
A1	Homopolymer	24	0.85	0.575	1.320	0.582	65
B1	High crystalline	22/86	0.84	0.584	1.337	0.591	44
B2	copolymers	13/132	0.92	0.586	1.348	0.592	53
B3		17/119	0.91	0.576	1.316	0.585	45
C1	Low crystalline	34/109	0.60	0.579	1.347	0.591	11
C2	copolymers	17/90	0.57	0.586	1.348	0.592	15
C3		156	0.39	0.573	1.329	0.591	19
C4		20/141	0.83	0.572	1.314	0.591	19

Notes: HW, azimuthal halfwidth (width at 0.5 of peak height). The numerator corresponds to relatively highly oriented crystallites, denominator to relatively weak oriented ones, where such separation was possible; f, orientation factor; a, b, c, unit cell parameters of the orthorhombic crystal lattice; C, degree of crystallinity.

that have transformed from helical to nearly planar zig-zag conformation. The authors have suggested that the β-phase was formed from the amorphous part of the polymer during uniaxial drawing at elevated temperatures.

In our opinion, the new structure cannot be attributed to a true polymer crystal with long-range 3D-order. The latter follows from an absence of meridional and quadrant reflections associated with this phase. Only a single intense equatorial maximum is observed (Fig. 3(e)), accompanied by weak broad streak-like scattering with diffusive character localized in the vicinity of the first layer line ($2\theta \sim 19°$). In our opinion, the specific scattering features of the β-phase rather point to a 2D mesomorphic structure with pseudohexagonal lattice characterized by random shifts of adjacent conformationally disordered chains along the macromolecular axis. This structure is similar to the 2D-pseudohexagonal mesophase first observed by Bassett [15] in linear PE heated under hydrostatic pressures above 4–5 kbars, from which extended-chain crystals are formed on subsequent cooling.

The mechanical properties of fibers prepared from PHA homo- and co-polymers under study can vary considerably, from values typical of high-modulus high-strength material to those characteristic of elastomers. Table 2 summarizes the results accumulated in the current study, together with some literature data used for reference.

Table 2
Mechanical properties of PHA materials under study, together with some reference data

Sample	E (GPa)	σ_{max} (MPa)	ε_{max} (%)	R (%)
A1	2.5	165	32	85
A2	3.9	172	33	93
A3	2.1	135	65	90
B1	200	57	310	65
B2	670	100	190	61
B3	254	76	230	89
B4	605	150	168	67
B5	1097	246	105	63
B6	1660	314	31	58
C1	20	34	2600[a]	88
C2	67	82	200	93
C3	290	59	4400[a]	64
C4	29	50	370	95
Hard-elastic POM fiber [16]	–	–	250	92 (at $\varepsilon=50\%$)
Hard-elastic PP fiber [16]	2.8	70	300	82 (at $\varepsilon=25\%$)
Hard-elastic PE fiber [17]	–	100	125	81 (at $\varepsilon=80\%$)
High-speed spun fiber [6]	5.8	228	72.2	–
	7.6	250	35.9	–
Melt spun fiber [6]	5.2	178	70.6	–
	7.7	330	37.2	–
Melt spun fiber [11]	2.2	109	160	–
	5.6	190	54	–
Isotropic film [18]	5	40	5	–

Notes: E, Young's modulus; σ_{max}, stress at break; ε_{max}, strain at break; R, reversibility factor measured for post-break relaxation of the samples—see Eq. (1) (values are for $\varepsilon=\varepsilon_{max}$ unless stated otherwise).

[a] The actual values of ε_{max} exceed those listed in the table; due to technical limitations of the testing machine, the break values of elongation for samples C1 and C3 were not reached.

Compared to isotropic samples, fibers of PHB homopolymer (type A) show a significant increase in tensile strength and elongation at break, while preserving high values of tensile modulus (Table 2). It is worth mentioning once again that since we have not yet optimized the fiber spinning conditions, the observed mechanical parameters are unlikely to be the best achievable; optimization of the procedure is expected to result in additional property improvement.

In spite of the perception of neat PHB being a brittle material at ambient temperature [18,19], we have shown that its gel-spun fibers with crystallinity close to that of isotropic PHB can undergo rather high deformations. In addition, we have found a feature relatively rarely observed for highly crystalline polymer materials—the high elasticity effect. More specifically, our PHB fiber with a crystallinity ~70% restores its longitudinal dimensions practically instantly, with residual deformation of only a few percent, after drawing to break at considerable strain (limiting value ε) (Fig. 4). Such behavior clearly points to 'hard-elastic' properties [16] of the PHB fibers produced, very much like those observed for some other polymers (see the references data in Table 2).

The usage of parameter R (recovery factor) instead of residual strain is known to be more reliable. Its values are also listed in Table 2. R is calculated from:

$$R = \frac{l_{max} - l_r}{l_{max} - l_0} \times 100\% = \frac{\varepsilon - \varepsilon_r}{\varepsilon} \times 100\%, \quad (1)$$

where l_{max} is the length of the drawn sample, l_r, length of the sample after recovery; l_0, the initial length; ε, the relative deformation; and ε_r, the relative residual deformation. Thus,

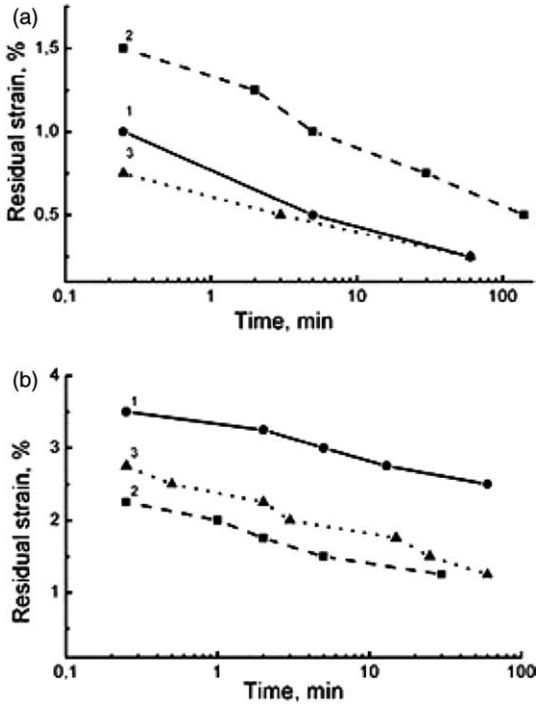

Fig. 4. Strain recovery of PHB fibers after unloading of the sample previously drawn to $\varepsilon=10\%$ (a) and 20% strain (b); A1 (curve 1), A2 (curve 2), A3 (curve 3)—fibers prepared under different processing conditions described in [8].

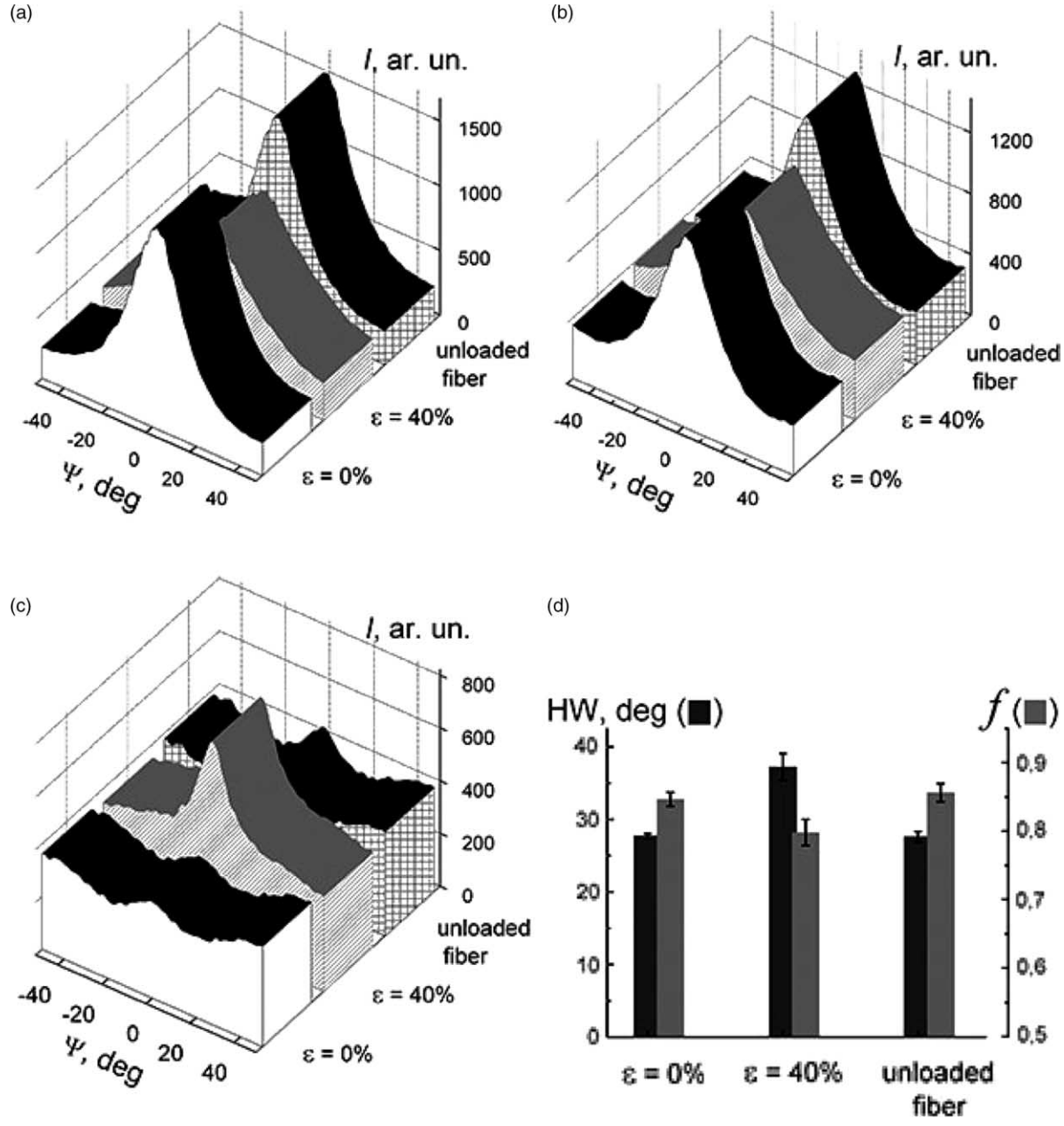

Fig. 5. Changes of azimuthal (Ψ) profiles of the orthorhombic (020) (a) and (110) (b) crystalline and (100) (c) mesophase equatorial reflections upon deformation of the PHB fiber (A-type); (d) azimuthal halfwidth (HW) and orientation factor (f) calculated from the meridional (002) Bragg spot.

$R = 100\%$ for a sample showing complete recovery after unloading, while $R = 0$ if no recovery takes place.

The relaxation behaviour observed for the gel-spun PHB fibers prepared looks at least commensurable with that of the 'traditional' hard-elastic polyoxymethylene (POM), PP and PE (Table 2). It should be noted that this is the first observation of hard-elasticity in these bacterial polyesters.

As it turned out, the relatively high-crystallinity fibers of PHA copolymers (type B) obtained by melt-spinning, possess mechanical characteristics, which compare well with those for industrial thermoplastics (Table 2). The wide variety of parameters observed is related to variations in processing conditions and subsequent treatment (annealing, additional drawing, etc.). The majority of the fibers under study display a combination of relatively high crystallinity with a unique ability for large reversible deformation, in a similar way as described for gel-spun PHB fibers. Moreover, fibers of the relatively low-crystallinity PHA copolymer (type C) exhibit practically rubber-like behaviour (Table 2), although they contain ~10–20% of crystalline phase (Table. 1).

Formally, one can classify the latter polymers as elastomers, in spite of their lack of chemical cross-links. It is likely that isolated crystals, distributed within the amorphous matrix, play the role of physical cross-links forming a 3D-network. Accordingly, these polymers belong to the class of thermoplastic elastomers or thermoelastoplastics [20]. It is important to appreciate the extraordinarily high values of elongation at break (sometimes up to a few thousand percents) for these

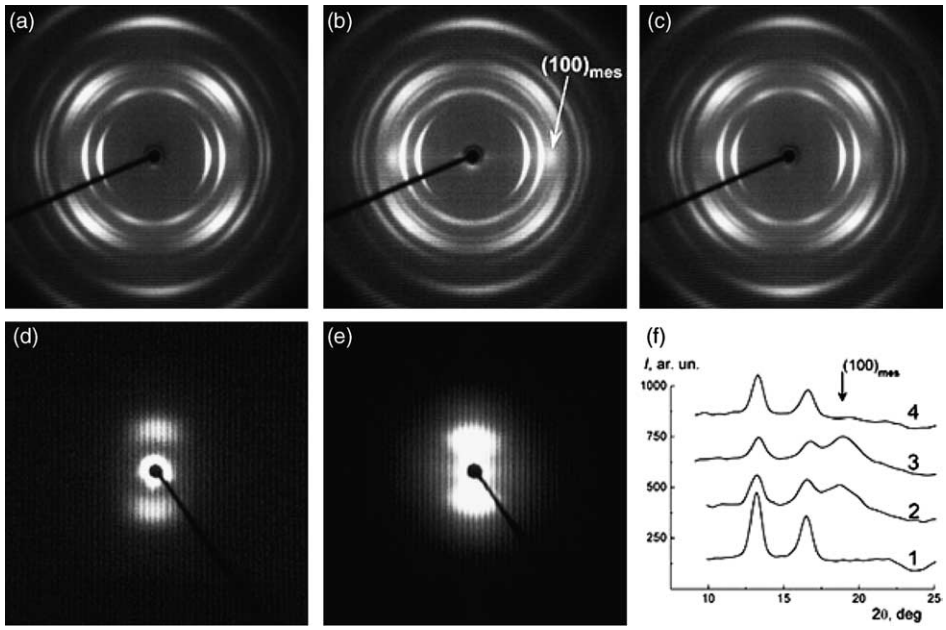

Fig. 6. WAXS (a–c) and SAXS (d and e) patterns recorded for the as-spun fiber (a and d), fiber drawn to $\varepsilon = 50\%$ (b and e) and subsequently unloaded (c) PHB fibers (A-type), as well as equatorial diffractograms (f) of initial PHB fiber (1), fiber drawn at 50 (2), 60% (3) and after subsequent unloading (4). Fiber axis is vertical.

copolymer fibers, exceeding or at least comparable to the values for true rubbers. What is especially striking is that upon unloading (or at break) the fibers instantly and almost completely restore their initial dimensions, thus exhibiting a combination of high extensibility and high elastic recovery from large extensions.

3.2. Strain-induced structural changes in PHA fibers

The unusual deformation properties of fibers of both neat PHB and its copolymers has motivated us to perform a comparative structural study of initial, strained (drawn and kept with fixed ends) and then unloaded relaxed fibers. X-ray diffraction experiments have revealed at least two non-trivial phenomena at ambient temperature. The first is the 'abnormal orientation effect'. Meridional (002) and equatorial (020) and (110) reflections were used for determining the degree of crystalline orientation in deformed PHB fibers. This was found to decrease, resulting in a change in the orientation factor f from 0.85 to 0.80 at $\varepsilon = 40\%$ (Fig. 5), Such behavior is in contrast to that normal in polymer fibers, where the situation is reversed. On the other hand, the behaviour observed here is typical of hard-elastic polymers, for example, hard-elastic PP [16]. The effect observed in the present study is reliably reproducible not only for homopolymer PHB but also for its high- and low-crystallinity copolymers. After unloading or break the degree of orientation reverts to its original higher value, indicating the reversible character of the effect observed (Fig. 5).

The second phenomenon found is a strain-induced phase transition. While in the initial state the PHB fibers contain only amorphous and crystalline phases, upon deformation of the fiber an additional reflection appears on the equator of the WAXS pattern at $2\theta = 18.7°$ ($d = 0.47$ nm). Its intensity increases with increasing elongation of the sample and it disappears after subsequent unloading (Fig. 6). The new Bragg spot corresponds to the 2D-pseudohexagonal packing of macromolecules in the mesomorphic state. Like the change in crystal orientation upon drawing, this phase transition is reversible. The residual deformation after unloading is very small (Table 2).

From the WAXS data (Table 3) one can see that under the deformation accompanied by the mesophase formation, crystal dimensions decrease reversibly, by ~1–2 nm, both in the longitudinal and transverse directions. At the same time, the angular position of the small-angle meridional reflection also changes reversibly (Fig. 6), which corresponds to an increase in long periodicity from 10 to 14 nm (Table 3). These observations suggest the possibility that deformation induces a reversible crystal to mesophase transition, whereby the mesophase is formed under loading not only from the amorphous material (as concluded in [14]), but partially also from the crystalline phase. However, this conclusion might be speculative, since it is not an easy task to truly measure

Table 3
Structural changes upon deformation of PHB fibers

Sample	L_{020} (nm)	L_{110} (nm)	L_{002} (nm)	L (nm)	HW_{020} (°)
Initial fiber	14.0	13.5	6.8	10	27.7
Fiber drawn to 30%	12.5	11.5	6.2	14	37.2
Unloaded fiber	13.5	13.6	7.1	–	27.6

Notes: HW_{020}, azimuthal halfwidth (width at 0.5 of peak height) for reflection (002); L_{020}, L_{110}, L_{002}, crystallite sizes along corresponding crystallographic directions; L, long periodicity.

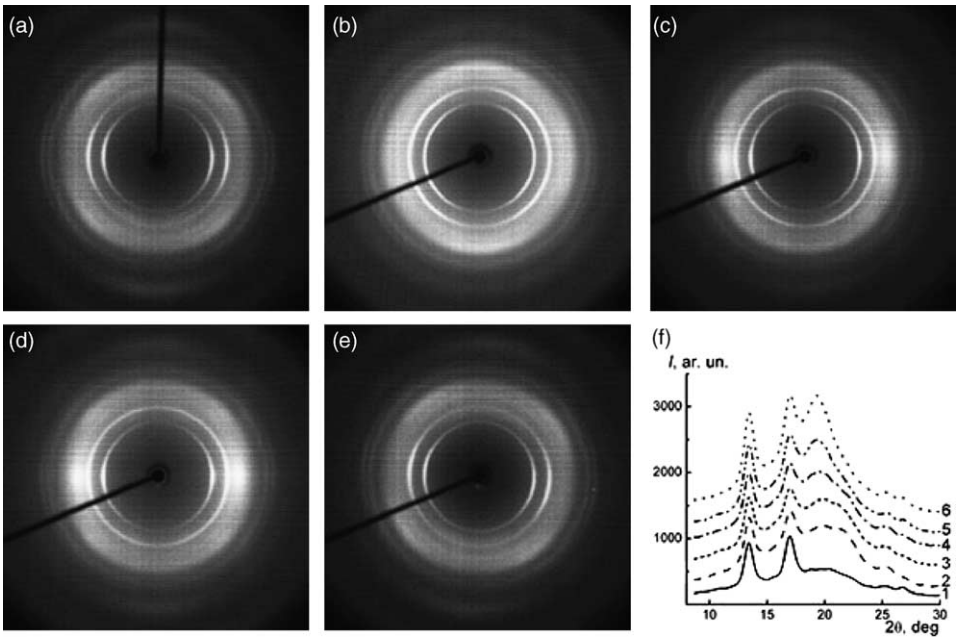

Fig. 7. X-ray patterns of the initial (a), deformed to 120% (b), 450% (c), 600% (d), and unloaded (e) low-crystallinity fibers (C-type). (f) Equatorial diffractograms at $\varepsilon = 0\%$ (1), 120% (2), 200% (3), 300% (4), 450% (5) and 600% (6) elongation. Fiber axis is vertical.

crystallinity of an oriented sample under strain, which is containing three phases.

Reversible formation of the mesophase is observed for all three families of materials under study, i.e. fibers of the homopolymer and of copolymer with different crystallinities. The only exception was fiber B4, which had already contained a mesophase component in the initial as-spun state due to high orientation drawing ($\lambda = 10$) applied during processing. Nevertheless, it has been established that the strain-induced mesophase formation can take place in this fiber as well (see below).

Interesting results are obtained for fibers prepared from the low-crystallinity copolymers (type C) that are characterized by the exceptionally high values of elongation at break (Table 2). For these samples, a pronounced mesophase reflection appears only when deformation exceeds 200% (Fig. 7). This is probably due to the fact that in these nearly amorphous polymers only preliminary extension of the initially Gaussian chains occurs at

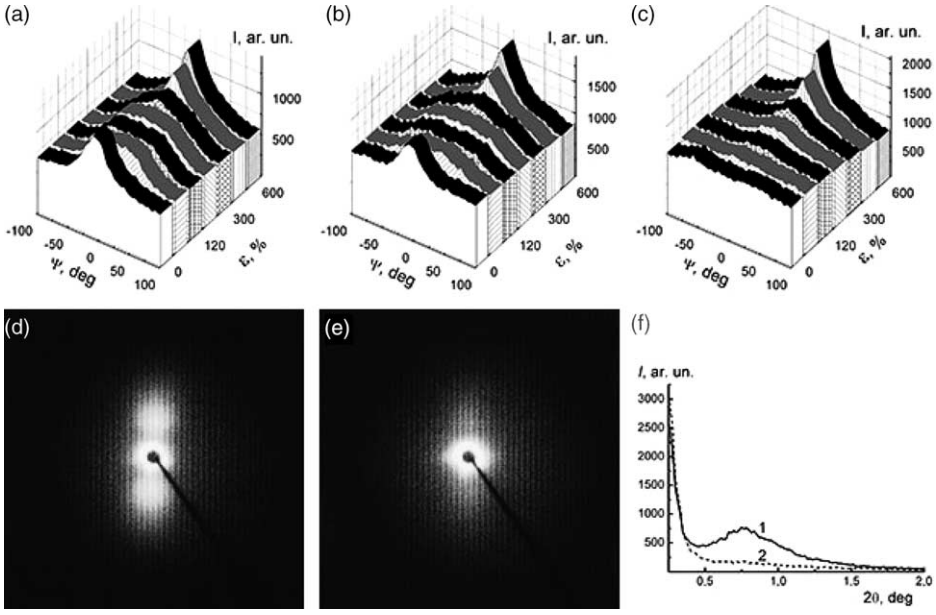

Fig. 8. Changes in azimuthal profiles upon deformation of the low-crystallinity fiber (C-type) measured on crystalline reflections (020) (a) and (110) (b), and on mesophase (100) reflection (c)/(d) SAXS pattern of the initial fiber and (e) of the fiber drawn at 450% elongation (fiber axis is vertical); (f), meridional diffractograms for the same initial (1) and drawn (2) fiber.

Table 4
Variation in azimuthal halfwidths of Bragg reflections upon C1 fiber drawing

ε (%)	f	HW (°)		
		020_{cr} ($2\theta \sim 13.1°$)	110_{cr} ($2\theta \sim 16.7°$)	100_{mes} ($2\theta \sim 18.7°$)
0	0.57	43 (143/39)[a]	38 (283/37)	–
67	0.48	91	97	–
120	0.45	104	116	55
200	0.44	105	121	57
300	0.46	95	96	52 (147/42)
450	0.50	47 (92/20)	52 (119/26)	37 (105/24)
600	0.52	38 (89/22)	43 (105/27)	27 (96/18)

Notes: ε, elongation; f, orientation factor; HW, azimuthal halfwidth (width at 0.5 of peak height) of the (020) reflection.
[a] The numerator corresponds to the relatively highly oriented crystallites, denominator to the relatively weak oriented ones, where such separation was possible.

the very beginning of drawing. On drawing above $\varepsilon = 200\%$ of the increasingly extended macromolecules pack on a 2D-pseudohexagonal lattice. At $\varepsilon \geq 200\%$, the mesophase content increases with increasing ε. Upon sample contraction after the removal of stress, the mesophase disappears, as described above for fibers of PHB homopolymers.

It is also of interest to note that the change in crystal orientation in the low-crystallinity copolymer fibers follows a rather complex pattern (Figs. 7 and 8, Table 4). At relatively low deformations, the parameter f decreases, as in the high-crystallinity PHB fibers. However, at deformations exceeding $\varepsilon \sim 200\%$, the overall degree of orientation increases again. The drop-like form of SAXS reflections in the small-angle X-ray patterns of low-crystallinity fibers (Fig. 8) suggests lamellar rather than fibrillar morphology.

From our viewpoint, such behaviour of the fibers indicates that the true hard-elastic mechanism of elasticity operates only at the first stage of drawing, up to $\varepsilon \approx 200\%$. The schematic representation of the morphological changes is shown in Fig. 9. The crystalline lamellae under strain deviate from the original orientation, initially perpendicular to the fiber axis, and become tilted as in the 'Chinese lantern' model of hard-elastic deformation proposed in [16]. Under the action of the mechanical field, the crystallites are tilted and displaced without any destruction. At higher deformation (the second stage), the 'usual' entropy effect starts work, when the 'random coil—extended chain' transition takes place. The observed at $\varepsilon \geq 200\%$ increase in overall degree of orientation is quite typical of this mechanism. Indeed, one can notice that the amorphous phase becomes oriented too at increasing drawing (Fig. 8(c); Table 4). The orientation is accompanied by an appearance of a certain fraction of extended fragments of macromolecular chains in amorphous areas with their ends fixed in crystallites. Obviously, namely these chain fragments form mesophase regions, which are destroyed during material relaxation after unloading. In the last column of Table 4, the highly and weakly oriented moieties correspond to the mesophase and the amorphous phase, respectively. It is seen that, when the tensile strain is increased, the azimuthal

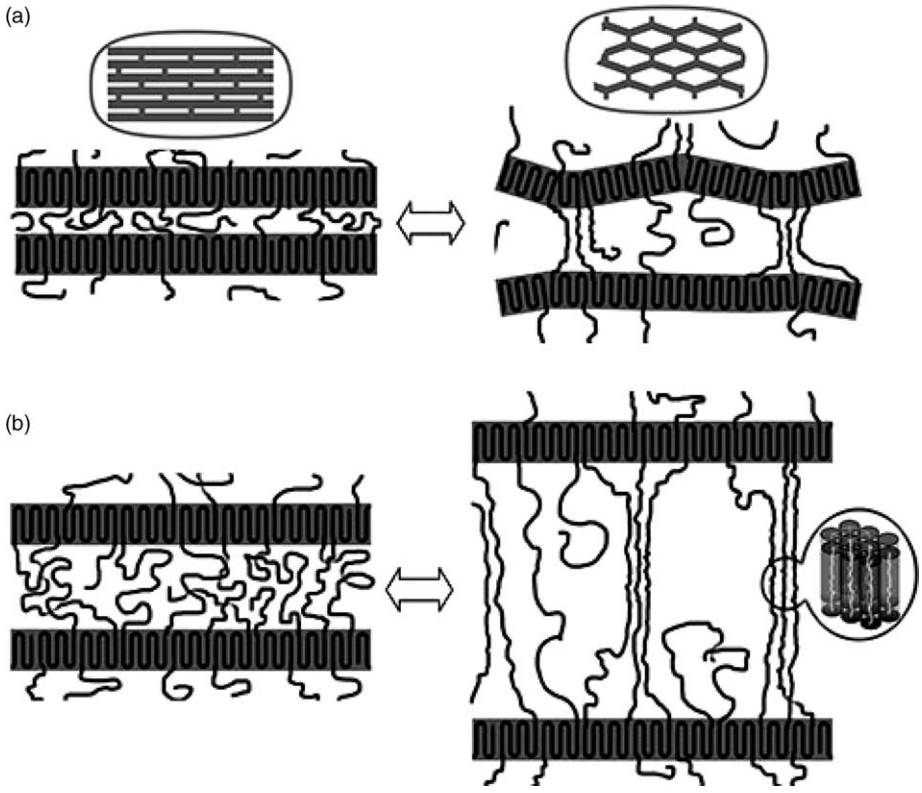

Fig. 9. Schematic representation of morphological changes in a PHA fiber under drawing: (a) $\varepsilon < 200\%$ (b) $\varepsilon \geq 200\%$.

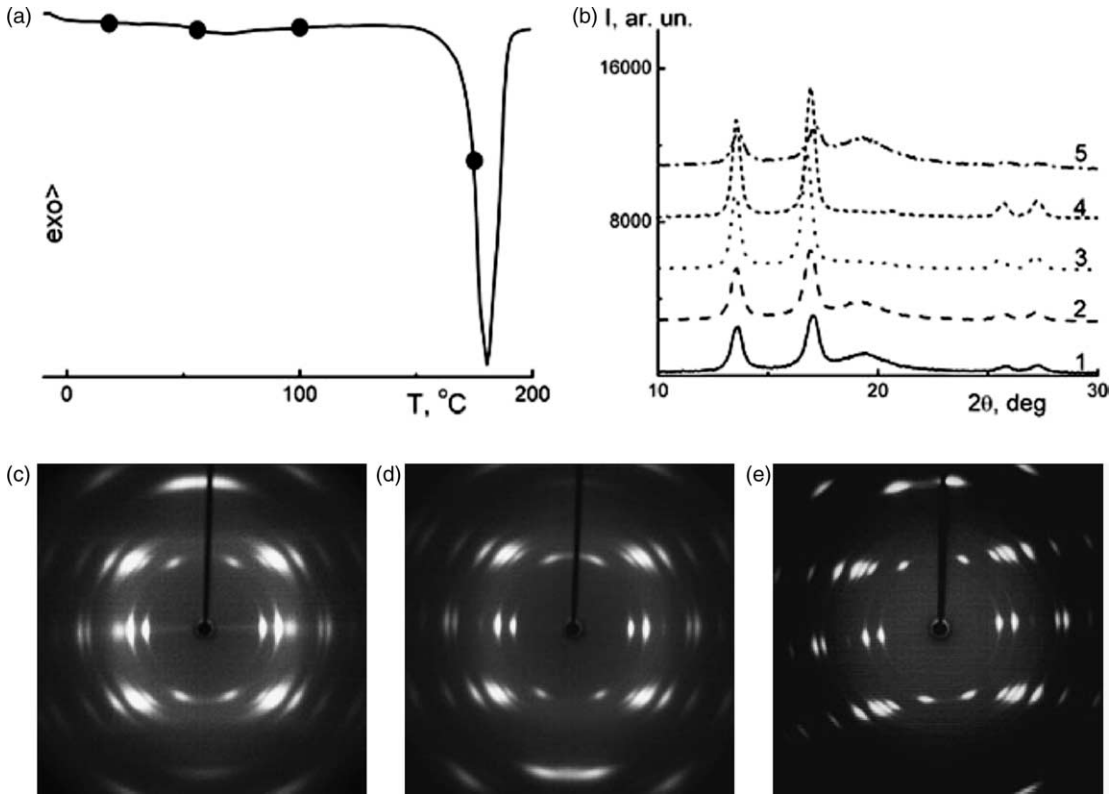

Fig. 10. DSC trace (1st heating run) for the high-crystallinity B-type copolymer fiber (a), its equatorial diffractograms (b) recorded at 25 °C (1), 56 °C (2), and 100 °C (3), and again at ambient temperature (4), as well as of the annealed fiber drawn to 100% elongation (5). WAXS patterns are also shown before annealing (c) and after thermal treatment at 100 °C (d) and 175 °C (e) (fiber axis is vertical).

halfwidth of the X-ray reflection at $2\theta \sim 18.7°$ decreases (Table 4, Fig. 8(c)), thus suggesting equalization of chain axis directions in the mesophase state.

3.3. Structural changes upon thermal treatment of PHA fibers

Another task of the current research work was examination of stability of the strain-induced mesophase in PHB based fibers. It is obvious from the coexistence of two phases (amorphous and crystalline), always observed in semicrystalline polymers below the melting point, that these systems cannot be treated as truly equilibrium. The coexistence of three phases (amorphous, mesomorphic and crystalline) complicates the situation even further. It is suspected that the mesomorphic state found in the present fibers is metastable [14].

To clarify this issue we performed annealing of fiber B4, which, as mentioned above, initially contained the mesophase component. The temperature of heat treatment was chosen based on DSC data (Fig. 10(a)). The first WAXS measurement was carried out below the weak endotherm (5 J/g) at 68 °C, the second one above this temperature but below the melting range, and the final one within the melting range at its low temperature flank. The fiber was kept with fixed ends (isometric conditions) and X-rays scattering from a constant irradiated volume was recorded at all temperatures. Thus, the integral intensity remains unchanged during the measurements.

According to WAXS data (Fig. 10(b)–(e)) the mesophase disappears at temperatures above 68 °C. It follows that the weak endotherm corresponds to melting of the mesophase. On the other hand, the degree of crystallinity, crystal dimensions and the degree of orientation increased (Table 5), in line with the usual behavior of semicrystalline polymer under thermal treatment. Thus, one can conclude that above its melting point the mesophase probably partly recrystallizes. If the fiber is cooled to ambient temperature, the mesophase does not re-appear. However, the reversible formation of the mesophase can be observed again upon redrawing the fiber

Table 5
Changes of some crystallographic parameters upon fibers annealing

Fiber	L_{020} (nm)	L_{110} (nm)	L_{002} (nm)	f	HW_{020} (°)
B4					
As-spun fiber	13.0	13.0	7.0	0.75	11.55
Annealed fiber (100 °C, 3 h)	15.5	14.0	9.5	0.78	9.20
C1					
Initial fiber	15.31	14.57	5.35	0.44	41.30
Fiber drawn at 200%	14.18	12.93	–	0.31	106.60
Drawn fiber after annealing at 90 °C	19.13	17.91	5.26	0.71	21.55

Notes: L_{020}, L_{110}, L_{002}, crystallite dimensions along corresponding crystallographic directions; f, orientation factor; HW_{020}, azimuthal halfwidth (width at 0.5 of peak height) of the (020) Bragg reflection.

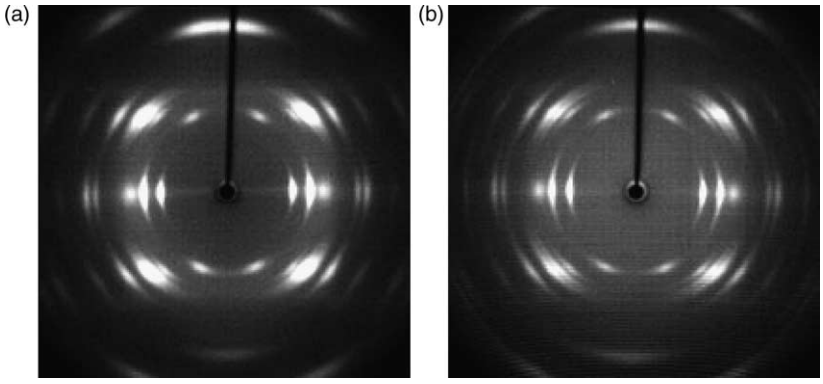

Fig. 11. WAXS patterns registered on 9.04.2003 (a) and 13.04.2004 (b) at ambient temperature for drawn high-crystalline fiber (B-type) kept with fixed ends.

previously annealed above the melting point of the mesophase. Such behavior is in agreement with the mechanism described above for PHB (Fig. 10(b), curve 5).

In our opinion, the latter proves that the mesophase always forms under deformation of the sample and is stable only under stress. Indeed, being kept at fixed ends, the drawn fiber does not change its structure and phase composition (including the mesophase content) for at least 1 year (Fig. 11). The mesophase can therefore be considered as mechanically induced.

In addition, to the disappearance of the mesophase and the increase in crystallinity, annealing close to the melting point ($T = 175$ °C) leads to additional improvement of crystal orientation (Fig. 10(e)). The calculated value of f is 0.75 for the initial sample, while for fibers annealed at 100 and 175 °C it increases to 0.81 and 0.84, respectively.

For comparison, we have performed similar heat treatment on PHB fibers that did not contain the mesophase initially. These samples were also found to go through increase of transverse crystallite dimensions, quantitatively comparable with those for the fiber described above. However, the changes in longitudinal crystal dimensions, measured from the halfwidth of the (002) reflection, show a clear difference—for the fibers without the mesophase in the initial state this change is estimated as 0.45 nm (from 9.95 to 10.4 nm) only, while for

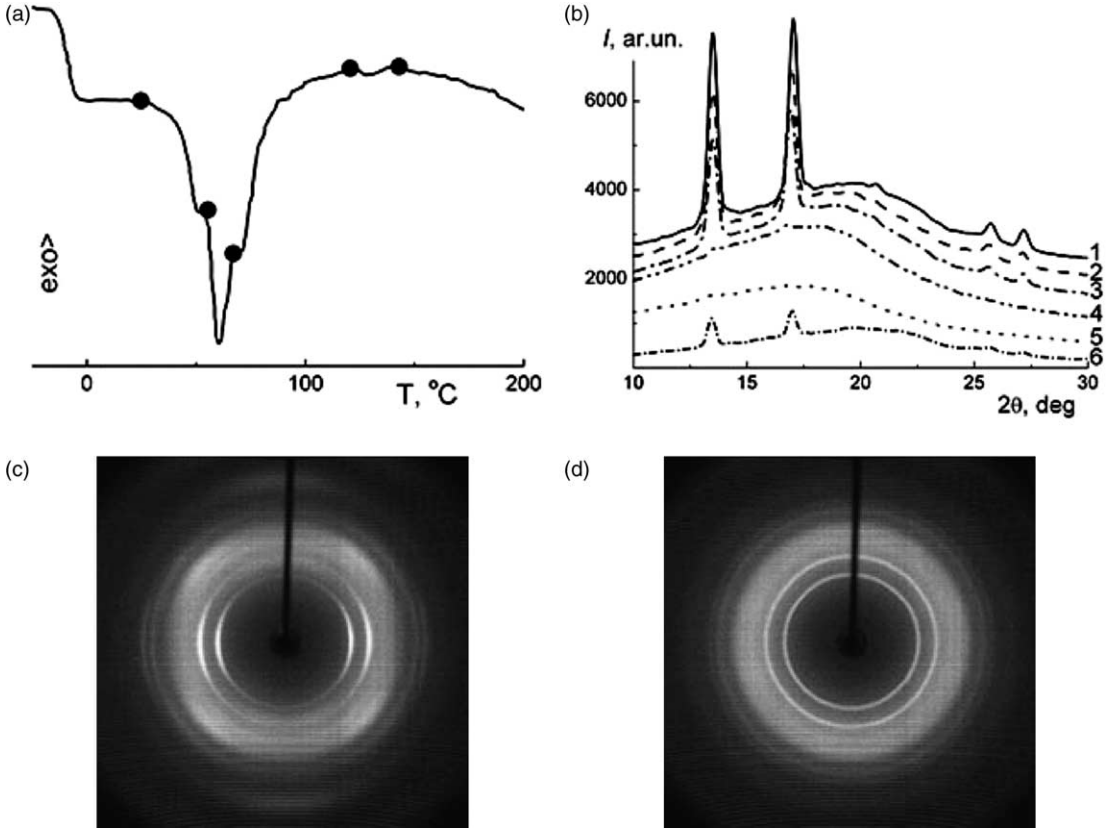

Fig. 12. DSC trace (1st heating) (a) for the as-spun low crystallinity fiber (C-type) and the equatorial diffractograms (b) obtained with fixed ends at 25 °C (1), 53 °C (2), 66 °C (3), 121 °C (4), 143 °C (5) and after subsequent cooling to 25 °C (6); (c) WAXS patterns registered before and (d) after fiber annealing at 100 °C (fiber axis is vertical).

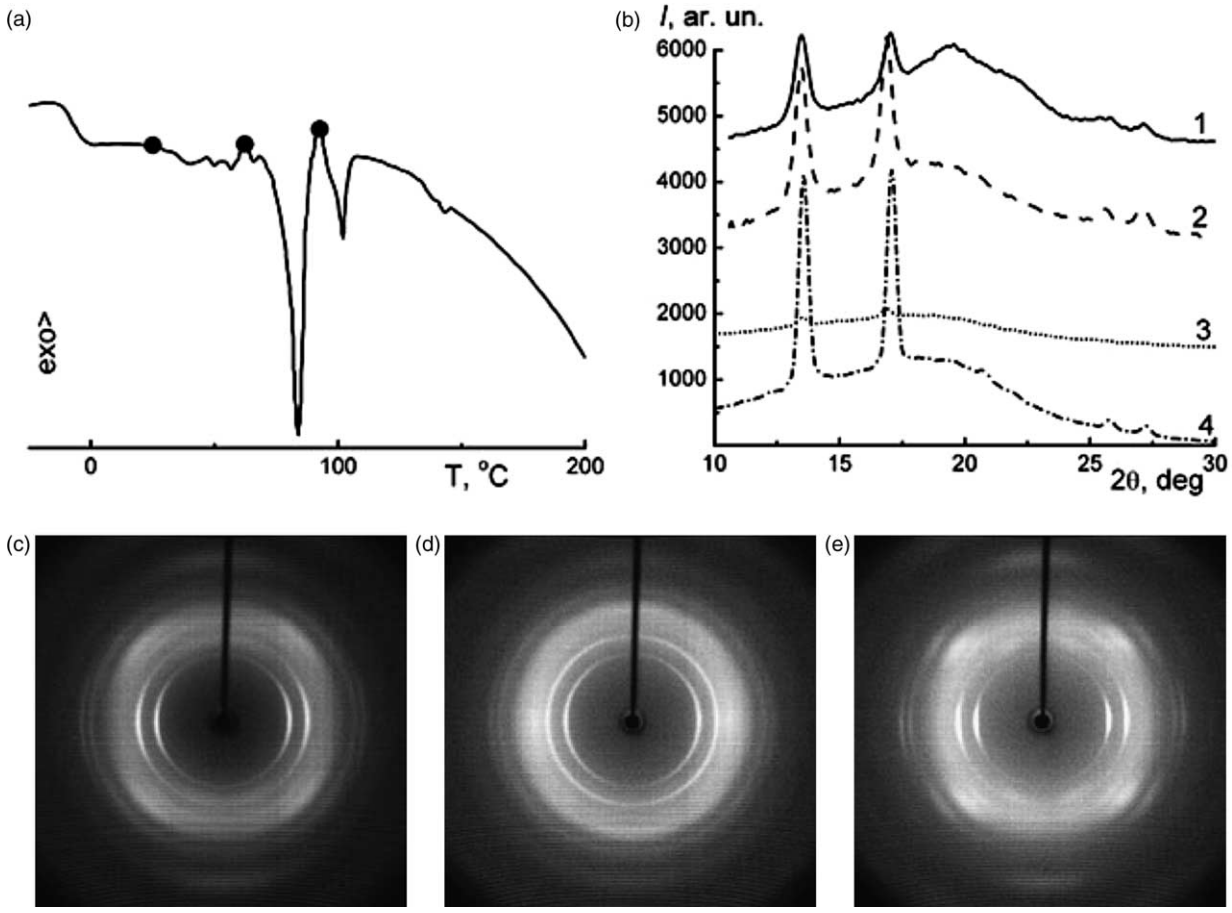

Fig. 13. DSC trace recorded for the low-crystallinity (C-type) fiber drawn to 300% and kept with fixed ends during the 1st heating run (a), equatorial diffractograms (b) recorded at 25 °C (1), 62 °C (2), 90 °C (3) and again at ambient temperature (4), and WAXS patterns of the initial fiber (c), and after drawing (d) and subsequent annealing at 90 °C (e) (fiber axis is vertical).

the fiber B4, initially containing the mesophase, it is 2.5 nm (from 7.0 to 9.5 nm) indicating that a mesophase to crystal transition occurred in the latter. Thus, the crystal thickness (dimension along fiber axis) increases because the mesophase–mesophase-amorphous stacks change to crystal–crystal-amorphous stacks.

The DSC traces recorded during the first heating run for the as-spun (Fig. 12(a)) and annealed (Fig. 13(a)) low-crystallinity fibers (C-type) are more complicated than those for PHB homopolymer and the high crystallinity copolymers. In order to clarify the situation, we performed a series of X-ray measurements at elevated temperatures (Figs. 12(b) and 13(b)) below the observed endotherms and within the temperature ranges between them. The fibers were always kept with fixed ends (both in X-ray and DSC experiments).

It was found for these as-spun fibers that heating does not lead to any substantial changes in the scattering profiles, except for the expected gradual decrease in diffraction intensity with temperature up to the melting point. One has to conclude that the complexity of the DSC traces (Fig. 12(a)) is not due to the presence of additional phases but to other effects such as multimodal distribution of crystal dimensions, lattice imperfections, coexistence of crystal with different orientations, etc. The decrease in Bragg reflection intensities after recrystallization from the melt (Fig. 12(b), curve 6, and (c) and (d)) is caused by the loss of preferred orientation and the redistribution of scattered intensity around the Debye rings. The overall degree of crystallinity remains the same upon recrystallization ($C \sim 15\%$).

The same fiber under deformation (at loading with strain $\varepsilon = 300\%$) was also examined at temperatures below and between the DSC endotherms (Fig. 13(a)). It was found that the weak endotherm at 40 °C corresponds to the disappearance of the mesophase (Fig. 13(b)). On heating up to 90 °C, i.e. somewhat above the strongest endotherm, crystal diffraction is still visible on the equator (Fig. 13(b), curve 3). Slow cooling during 30 min to ambient temperature produced unexpectedly high intensity of the equatorial crystalline reflections (Fig. 13(b), curve 4, and (e)). One can see also that annealing at 90 °C followed by cooling leads to an increase in crystal dimensions and in the degree of orientation (Table. 5 and Fig. 13(c)–(e)). At the same time, crystallinity remains practically unchanged at ~15%.

Only at heating above 105 °C, the material melts as a whole. Such behaviour justifies our assumption about coexistence of at least two sets of crystallites with different

dimensions resulting in the observation of two different melting temperatures in the DSC-trace. Apparently it can be explained by the fact that upon heating to 90 °C the largest and most-oriented along the fiber axis crystallites are still remaining. During the subsequent cooling from this temperature range the liquid phase of polymer material crystallizes with the remaining large crystallites using them as crystallization nuclei. This causes the resulting orientation growth.

4. Conclusions

The results of this work can be summarized as follows:

(i) The new approach, gel-spinning, was successfully applied in the processing of regular PHB, in order to obtain highly oriented fibers In this biodegradable polymer melting and degradation temperatures coincide, rendering melt-spinning difficult. However, traditional melt spinning can be recommended for processing of random copolymers based on PHB. These materials exhibit a relatively wide temperature window between melting and degradation temperatures, suitable for melt processing.

(ii) For the first time hard-elastic properties were found for PHA fibers. The highly crystalline PHB homopolymer and its random copolymers with relatively low comonomer content display true hard-elastic behaviour, whereas the relatively low crystallinity copolymers with high comonomer content behave rather like rubber.

(iii) A third phase, additional to the crystalline and amorphous phases, was identified in the PHA fibers under investigation. This is a columnar mesophase (or condis-crystal) with 2D-pseudohexagonal packing of macromolecular central axes The polymer chains are likely to be conformationally disordered.

(iv) The strain-induced reversible formation of the mesophase was observed for the first time in oriented PHA homopolymer and copolymer fibers. The mesophase develops on drawing above a critical elongation at ambient temperature and disappears on subsequent unloading.

(v) It was proven that the strain-induced mesomorphic state observed in PHA fibers is a thermodynamically stable phase formed only under mechanical stress, which seems to be the necessary condition for its existence. It is stable at temperatures $T \leq T_{\text{mes.melt.}} = 69$ °C, allowing it to be classified as mechano-thermotropic, in analogy with baro-thermotropic, first proposed by Bassett for polyethylene melted under high pressure [15].

Acknowledgements

We thank Prof. Dr T.G. Volova, Dr G.A. Bonartseva (Russia) and 'Metabolix Ltd' (USA) for providing the PHA samples for this study. Special thanks are due to Dr G.A. Bonartseva for the micrographs of the bacteria provided for this paper. Financial support by INTAS (grant no. 00-0525) and RFBR (project no. 03-03-32576) is also gratefully acknowledged.

References

[1] Braunegg G, Lefebvre G, Genser KF. J Biotechnol 1998;65:127.
[2] Lemoigne M. Bull Soc Chim Biol 1926;8:770.
[3] Sudesh K, Abe H, Doi Y. Prog Polym Sci 2000;25:1503.
[4] Rebrov AV, Dubinsky VA, Nekrasov YuP, Bonartseva GA, Stamm M, Antipov EM. Vysokomol Soedin 2002;44:347 [Polym sci B 2002;44:347].
[5] http://www.metabolix.com
[6] Schmack G, Jenichen D, Vogel R, Tandler B. J Polym Sci, Polym Phys 2000;38(21):2841.
[7] Dijkstra DJ, Pennings AJ. Polym Bull 1988;18:73.
[8] Gordeyev SA, Nekrasov YuP, Shilton SJ. J Appl Polym Sci 2001;81:2260.
[9] Bonartseva GA, Myshkina VM, Nikolaeva DA, Rebrov AV, Gerasin VA, Makhina TK. Microbiology (Russian) 2002;71(2):258.
[10] Volova TG, Lukovenko SG, Vasilyev AD. Biotechnology (Russian) 1996;1:19.
[11] Gordeyev SA, Nekrasov YuP. J Mater Sci Lett 1999;18(20):1691.
[12] Avella M, Martuscelli E, Raimo M. J Mater Sci 2000;35:523.
[13] Furuhashi Y, Ito H, Kikutani T, Yamamoto T, Kimizu M, Cakmak M. J Polym Sci, Part B: Polym Phys 1998;36:2471.
[14] Orts WJ, Marchessault RH, Bluhm TL, Hamer GK. Macromolecules 1990;23(26):5368.
[15] Basset DC, Turner B. Nat Phys Sci 1974;240(18):146.
[16] Cannon SL, McKenna GB, Statton WO. J Macromol Sci, Macromol Rev 1976;11:209.
[17] Miles M, Petermann J, Gleiter H. J Macromol Sci, Phys 1976;B12(4):523.
[18] De Koning GJM, Lemstra PJ. Polymer 1993;34:4089.
[19] De Koning GJM, Scheeren AHC, Lemstra PJ, Peeters M, Reynaers H. Polymer 1994;35(21):4598.
[20] Konyukhova EV, Neverov VM, Godovsky YuK, Chvalun SN, Soliman M. Macromol Mater Eng 2002;287:250.